Catalysis Science & Technology

Accepted Manuscript

ROYAL SOCIETY OF CHEMISTRY

www.rsc.org/catalysis

Journal Name

ARTICLE

Strong or weak acid, which is more efficient for Beckmann rearrangement reaction over solid acid catalysts?**.

Received 00th January 20xx,
Accepted 00th January 20xx

DOI: 10.1039/x0xx00000x

www.rsc.org/

Yueying Chu,[a] Peng Ji,[b] Xianfeng Yi,[a] Shenhui Li,[a] Peng Wu,[b] Anmin Zheng,*[a,c] Feng Deng*[a]

The effects of Brønsted acid strength and pore confinement on the Beckmann rearrangement (BR) reaction over solid acid catalysts have been explored. With the help of catalytic evaluation experiments, it is demonstrated that oximes with different size (cyclohexanone oxime and acetoxime) exhibit quite different BR reactivity dependence on the acid strength over microporous and mesoporous zeolites. In order to reveal the origin of such a difference, electronic structure calculations and kinetic analysis were performed. It's theoretically found that the confinement effect from microporous zeolite framework has more significant influence on the rate-determination step of BR reaction when the oxime reactant is well-confined inside the microporous voids, which in return controls the BR reactivity.

Introduction

Beckmann rearrangement (BR) reaction is a typical acid-catalyzed reaction to convert oxime to amide, and one of its most successfully commercialized applications is the conversion of cyclohexanone oxime to ε-caprolactam which is a valuable feedstock in the production of Nylon-6 and other resins. Conventionally, strong liquid acids, such as concentrated oleum and sulfuric acid, are utilized for the BR reaction and they exhibit relatively higher activity toward the reaction compared with weak liquid acids[1]. Solid acid catalysts (i.e., zeolites, metal oxides, and heteropoly acids etc) are of great interest due to their environmentally friendly properties, and they have been extensively used in the BR reaction in the past decades as well[2, 3, 4, 5, 6, 7]. Compared to the liquid acids, the non-corrosive solid acid catalysts are easier to recycle and don't emit harmful gas or waste during the catalytic process[8, 9, 10, 11]. Therefore, the BR reaction over solid acid catalysts has been the subject of intense research from both the fundamental studies and industrial applications.[12, 13, 14, 15]

Different from the liquid acid-catalyzed BR reaction where stronger acid favours its catalytic performance, how the acid strength influences the BR reactivity is still elusive for solid acid catalysts. For amorphous metal oxide catalysts, it was found that strong Brønsted acid sites facilitate the BR reaction. For example, Reddy and Mao demonstrated that boria catalysts supported on a titania-zirconia complex oxide (having strong acid sites) exhibit a higher BR catalytic performance in comparison with boria catalysts supported on a titania or zirconia oxide (having weak acid sites)[13, 16]. Similarly, excellent conversion and selectivity were achieved in the BR reaction of cyclohexanone oxime over mesoporous zeolites with strong acid sites. Compared with the weakly acidic Al-SBA-15 and Al-MCM-41 mesoporous zeolites, it was revealed that the BR reactivity was considerably enhanced after modification of the mesoporous catalysts with strong sulphonic-acid groups[17, 18, 19]. However, for microporous zeolite catalysts, many experimental results have demonstrated that weak acid sites are responsible for the high BR reactivity of cyclohexanone oxime[20, 21]. For example, Fois and his coworkers found by using IR spectroscopy that although both weakly acidic silanols in silicalite-1 and strong acidic bridging hydroxyl groups in zeolite H-ZSM-5 could catalyze the BR reaction of cyclohexanone oxime, the reaction at the weak acidic sites has a much lower activation barrier through a mechanism not involving a protonated intermediate[20]. Raja et al have also illustrated that weaker acidities of MgSiAlPO-5 molecular sieve will result in considerably superior performance for the cyclohexanone oxime BR reaction than the relatively stronger acidic MgAlPO-5 catalyst.[22] Obviously, solid acid catalysts with different framework structures (such as microprous and mesoporous zeolites) exhibit quite different BR activity upon the acid strength.

In order to gain insight into the influence of Brønsted acid strength on the BR catalytic performances, we used catalytic experiments and DFT calculations to explore the reactions of oxime with different molecular size (cyclohexanone oxime and acetoxime) on solid acid catalysts with different pore size (microporous ZSM-5 and mesoporous MCM-41 zeolites) and

[a] State Key Laboratory of Magnetic Resonance and Atomic and Molecular Physics, National Center for Magnetic Resonance in Wuhan, Wuhan Institute of Physics and Mathematics, Chinese Academy of Sciences, Wuhan 430071 (P.R. China) Fax: (+) 86-27-87199291. Email: zhenganm@wipm.ac.cn; dengf@wipm.ac.cn
[b] Key Laboratory of Green Chemistry and Chemical Processes, Department of Chemistry, East China Normal University, Shanghai 200062 (P.R. China)
[c] Hubei Key Laboratory for Processing and Application of Catalytic Materials, Huanggang Normal University, Huanggang 438000 (P.R. China)

† Supplementary Information (ESI) available: Experimental details, the activation barriers of the Beckmann reactions over the 8T cluster models with varying acid strength, and the corresponding optimized TS structures. See DOI: 10.1039/x0xx00000x

varied acid strength (Si-, B-, and Al-substituted microporous and mesoporous zeolites with a successively increased acid strength[21]). We found experimentally that cyclohexanone oxime and acetoxime show quite different BR reactivity dependence on the acid strength over microporous and mesoporous zeolites. Furthermore, theoretical calculations have revealed that the pore confinement effect from the zeolite framework has a more significant influence on the rate-determination step of BR reaction when the oxime reactant is well-confined inside the microporous voids, which in return determines the catalytic performance.

Catalytic experiments

The BR reactions of cyclohexanone oxime and acetoxime were carried out under atmospheric pressure in a quartz tube reactor (8 mm i.d. and 600 mm length). The catalyst (0.4 g, 20–40 mesh size) was loaded in the reactor and subjected to activation in a nitrogen stream at 683 K (for cyclohexanone oxime) and 703 K (for acetoxime) for 0.5 h. Then, the catalyst was regulated to a selected temperature for reaction. Firstly a solution of cyclohexanone oxime or acetoxime in ethanol (15 wt. %) was injected using a syringe pump under a nitrogen flow (25 mL min-1). The weight hourly space velocities (WHSV) of cyclohexanone oxime and acetoxime are both 3.5 h^{-1}. The products and remaining reactants were collected with an ice/water trap, and were analyzed by gas chromatography (Shimadzu 2014) equipped with a DM-WAX capillary column (30 m × 0.25 mm × 0.25 mm) and a FID detector.

Theoretical calculations

It is well-accepted that the Beckmann rearrangement reaction is a typical Brønsted acid-catalyzed reaction [13, 14, 21, 23, 24]. In the presence of Lewis acid (such as extra-framework Al species) in zeolites, its synergy with the Brønsted acid will lead to an enhanced acid strength of Brønsted acid[25]. Therefore, the effect of Lewis acid sites on the BR reaction was not taken into account in this work. The Brønsted acidity could be mimicked by tuning the terminal Si–H bonds of zeolite models in theoretical calculation[26, 27, 28]. An 8T HZSM–5 cluster model with different terminal Si–H bond length to represent a series isolated acid sites with different acid strengths. It's noteworthy that the confinement effect derived from the microporous zeolite was not taken into account for this simplified 8T cluster, therefore, such models can be used to represent the acidic properties of mesoporous zeolites (such as MCM-41 and SBA-15) or amorphous metal oxides. In the calculations, the 8T model was cut out of the crystallographic structure of H-ZSM-5 zeolite[29], and the Al12–O24H–Si12 site was used to represent the Brønsted acid site. All terminal hydrogen atoms in the calculated cluster were defined to locate at a distance r_{Si-H} away from the corresponding silicons during calculations, so that each Si–H bond is oriented along the direction toward the neighboring oxygen atom. As such, Brønsted acid sites with different acidic strengths can readily be represented by varying the r_{Si-H} value in the 8T cluster model. The calculations were performed using ωB97XD hybrid density function with 6-31G(d, p) basis sets. The boundary SiH_3 groups of the cluster

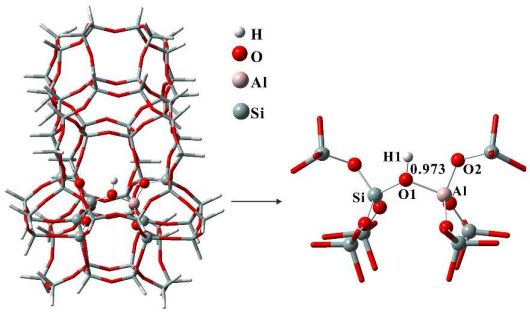

Figure 1 Representation of zeolite H-ZSM-5 framework structure by a 72T cluster model (viewing along the [1 0 0] direction). The 8T cluster represented as ball and stick view was treated as the high-layer atoms during the ONIOM calculations.

model were fixed, while other atoms of the acid site model and the organic fragment were allowed to relax during the structure optimizations. In the calculation, the activation barrier (E_{act}) is calculated as the energy difference between the absorption complex and transition state of the guest–host systems, i.e., $E_{act} = E_{TS} - E_{ads}$.

H-ZSM-5 zeolite with complete pore structure is used as a model to investigate the influence of the zeolite framework on the reactivity of the Beckmann rearrangement reaction. An extended 72T cluster model consisting of a complete 10-MR channel and one Brønsted acid site (see Figure 1) was adopted to represent the H-ZSM-5 zeolite, and the reliability has been confirmed by the agreement of the adsorption structure and energies predicted by such 72T model and the experimental results of pyridine molecules trapped inside the zeolite H-ZSM-5 [30]. The structure parameters adopted during the calculations were extracted from the crystallographic structural data of ZSM-5[29] . The terminal Si–H was fixed at a bond length of 1.47 Å, oriented along the direction of the corresponding Si–O bond. The combined theoretical model, namely ONIOM (ωB97XD/6-31G(d,p):MNDO) was applied to predict the geometries of various adsorption structures and transition states. To preserve the integrity of the zeolite structure during the structure optimizations, only the $(SiO)_3$–Si–OH–Al–$(SiO)_3$ activated center and adsorbed molecules in the high-level layer are relaxed while the rest of atoms are fixed at their crystallographic locations. In order to obtain accurate energy data, the single point energies calculations were further refined at the level of ωB97XD /6-31G(d, p). All the geometry optimizations and frequency calculations were performed using the Gaussian 09 package [31].

For visualizing the noncovalent interactions between the adsorbed organic species and the zeolite pore, the noncovalent interaction index approach, developed by Yang et al.[32], was adopted. In this approach, the reduced density gradient (RDG), defined as $s= (1/(2(3\pi^2)^{1/3}))((|\Delta\rho(r)|)/(\rho(r)^{4/3}))$, together with the electron density ρ, was used to distinguish the covalent and noncovalent interactions. The noncovalent interactions locate in the regions with low density and low RDG. The sign of the second largest eigenvalue (λ_2) of the electron density Hessian can be used to distinguish bonded ($\lambda_2 < 0$) from nonbonded ($\lambda_2 > 0$) interactions.

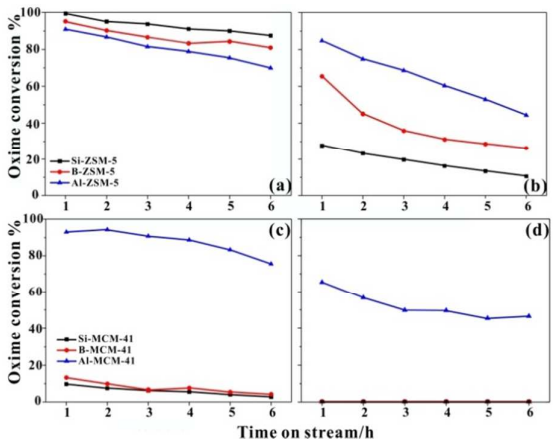

Figure 2. Conversion of cyclohexanone oxime (a,c) and acetoxime (b，d) as a function of time on stream in BR reaction over MFI-type (a, b) and MCM-14-type (c, d) zeolites with varied acid strengths at 633 K (for cyclohexanone oxime) and 653 K (for acetoxime).

The analysis of the sigh of λ_2 can help to discern different types of noncovalent interactions: (sign(λ_2)ρ < 0, H-bonding interaction; sign(λ_2)ρ≈0, weak van der Waals (vdW) interaction and sign(λ_2)ρ > 0, strong repulsive interaction). To exhibit the intermolecular noncovalent interaction between the adsorbed organic fragment and the zeolite framework more obviously, the intramolecular interactions are eliminated for the calculated RDG function. The functions RDG and sign(λ_2)ρ were calculated with the Multiwfn software[33].

Result and discussion

Catalytic Experiments of BR reaction on zeolites with different compositions

It was demonstrated that the acid strength of microporous ZSM-5 zeolites with different compositions follows the order: Al-ZSM-5>B-ZSM-5>Si-ZSM-5[21], and the similar order was observed for the mesoporous MCM-41 samples [34, 35]. Figure 2 shows oxime conversions as a function of time on stream at 1 h^{-1} WHSV over MFI-type and MCM-14-type zeolites with different compositions. The textural properties of zeolites and the corresponding catalytic data were listed in Table S1 and Table 1 respectively. When the BR reaction of cyclohexanone oxime was carried out at 633 K, Si-ZSM-5 with the weakest strength (solely having silanol group) shows the highest conversion among the three MFI-type zeolites, and the lowest conversion is observable for Al-ZSM-5 with the strongest acid strength (having Brønsted acid site, SiOHAl) (Figure 2a). The decreased conversion of oxime with the increase of acid strength demonstrates that weak acid could facilitate the cyclohexanone oxime conversion over the ZSM-5 zeolites. In addition, the caprolactam selectivity also exhibits a similar trend towards acid strength, which follows the order: Si-ZSM-5 > B-ZSM-5 > Al-ZSM-5 (see Figure S1a and Table 1). However, when the BR reaction of cyclohexanone oxime occurs on MCM-41-type mesoporous zeolites, the strongest acidic Al-MCM-41 shows the highest conversion and selectivity (see Figures 2c and S1c), while the weakest acidic Si-MCM-41 exhibits the lowest conversion and selectivity, which is quite different from the trend of microporous MFI-type zeolites.

The catalytic performance of small acetoxime over ZSM-5 was evaluated at 653 K as well. In contrast to cyclohexanone oxime

Table 1. A summary of Beckman rearrangement reaction of cyclohexanone oxime and acetoxime on ZSM-5 and MCM-41 catalysts with different compositions.

No.	Cat.	Si/B or Si/Al ratio	Cyclohexanone oxime rearrangement (%) [a]		Acetoxime rearrangement [b]	
			conv.	lactam sel.	conv.	lactam sel.
1	Si-ZSM-5	∞	99.4	96.2	27.8	86.4
2	B-ZSM-5	28	95.3	93.1	65.4	82.1
3	Al-ZSM-5	29	90.9	87.3	84.8	71.6
4	Si-MCM-41	∞	9.8	50. 7	27.6 [c]	72.4 [c]
5	B-MCM-41	27	13.4	47.2	57.2 [c]	66.3 [c]
6	Al-MCM-41	29	93. 0	78.7	65.4	74.3

[a] Evaluated at 633 K, TOS = 1 h.
[b] Evaluated at 653 K, TOS = 1 h.
[c] Evaluated at 733 K, TOS = 1 h. Si-MCM-41 and B-MCM-41 were almost inactive at 653 K for acetoxime rearrangement.

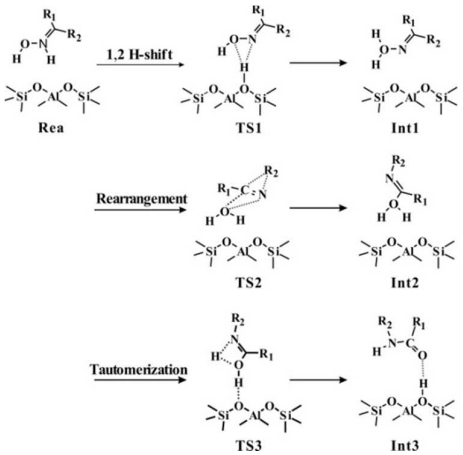

Scheme 1. The reaction mechanism of the Beckmann rearrangement.

where the most excellent reactivity is achieved over the weakest acidic Si-ZSM-5, the strongest acidic Al-ZSM-5 shows the highest acetoxime conversion (Figure 2b) and amide selectivity (Figure S1b), while the lowest conversion and amide selectivity are observable over the Si-ZSM-5 zeolite. This experimental result clearly indicates that strong acid could considerably promote the acetoxime conversion over MFI-type zeolites. It is noteworthy that although the BR reaction of acetoxime can occur on Al-MCM-41 at 653 K, Si- and B-substituted MCM-41 zeolites are almost inactive for the reaction under the same reaction condition (Figure 2d). When the reaction temperature was raised to 733 K, the Si- and B-substituted MCM-41 zeolites are active for the acetoxime BR reaction with the latter having a much higher acetoxime conversion (see Table 1).

On the basis of the aforementioned catalytic experiments, it's revealed that a stronger acid site leads to a higher BR reactivity for both acetoxime and cyclohexanone oxime in mesoporous MCM-41 zeolites, and for acetoxime in microporous ZSM-5 zeolites. However, a distinct result is obtained for the cyclohexanone oxime BR reaction over ZSM-5 zeolites that the most excellent reactivity is achieved over the weakest acidic Si-ZSM-5. Apparently, the acid strength is not the sole factor to determine the BR reactivity. Indeed, the most obvious difference between ZSM-5 and MCM-41 is their pore dimension size. Compared to ZSM-5 with a pore channel of ca. 0.55 nm, MCM-41 used here has a much larger pore dimension (2.6 nm). Since the molecular size of cyclohexanone oxime is comparable to the pore size of ZSM-5 but much smaller than that of MCM-41. Therefore, apart from the acid strength of zeolites, the pore confinement effect may be another key factor to determine the BR reactivity.

Theoretical investigations of the influence of Brønsted acid strength on the catalytic performance of BR Reaction

DFT theoretical calculation is a powerful approach to investigate the local structure and reaction mechanism of

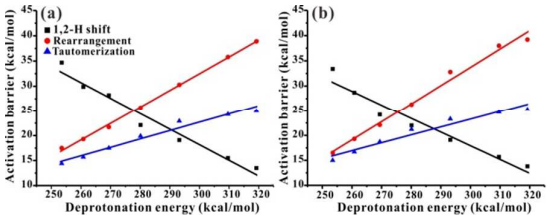

Figure 3. Dependences of BR activation barriers of cyclohexanone oxime (a) and acetoxime (b) on Brønsted acid strength (characterized by deprotonation energy).

zeolite catalysts[36, 37, 38, 39, 40, 41, 42]. An 8T cluster model with varied Brønsted acid strength (from weak, medium-strong, and strong to superacid, which is evaluated by its deprotonation energy, DPE) was used to explore the influences of Brønsted acid strength on the BR reaction[26, 27, 28]. It's noteworthy that such a simplified 8T model can solely represent the local structure and the acid strength of acid sites, but no confinement effect imposed by the pore structure of catalysts is taken into account.

The commonly mechanism of Beckmann reaction contains three element steps (see scheme 1): (1), 1,2-H shift step involves the transfer of the acidic proton H1 of catalysts from N-ended site to O-ended site; (2) rearrangement step corresponds to the migration of the R2 group to the N atom and the binding of H_2O to the C atom; (3) tautomerization step involves the transfer of a H atom from the OH group to N atom[43]. The transition state (TS) structure and activation barrier of BR reaction of the two oximes on the acidic protons with varied acid strength are shown in Figure S3-S7 and Table S2-S3, and Figure 3 displays the dependences of calculated activation barriers of the three element steps on the acid strength.

It can be seen from Figure 3a that increasing the acid strength from weak (DPE=319 kcal/mol) to mediate strong acid (DPE=276 kcal/mol, which is similar to the acid strength of $H_6CoW_{12}O_{40}$ heteropoly acid[44]), the rearrangement reaction (step 2) is the rate-determination step with an activation barrier being dramatically decreased from 38.9 to 25.7 kcal/mol, indicating that the BR reactivity could be linearly enhanced in this acid strength range. However, as the acid strength is further increased to stronger acid range (DPE < 276 kcal/mol), the reaction rate is determined by the 1, 2-H shift step (step 1), and the activation barrier of this step is gradually increased with the increase of acid strength. When the acid strength is increased to super acidity (DPE=253.5 kcal/mol, being similar to the acid strength of $H_3PW_{12}O_{40}$ heteropoly acid with a DPE of 259 kcal/mol)[44], the activation barrier of 1, 2-H shift step goes up to 34.7 kcal/mol. Therefore, it's revealed that a strong solid acid (with a DPE of ca. 276 kcal/mol) is the most efficient candidate for the BR reaction of cyclohexanone oxime. Figure 3b displays the activation barriers of the three primary steps as a function of acid strength for the BR conversion of small acetoxime. Almost the same trend is observable in which the rearrangement step is rate-

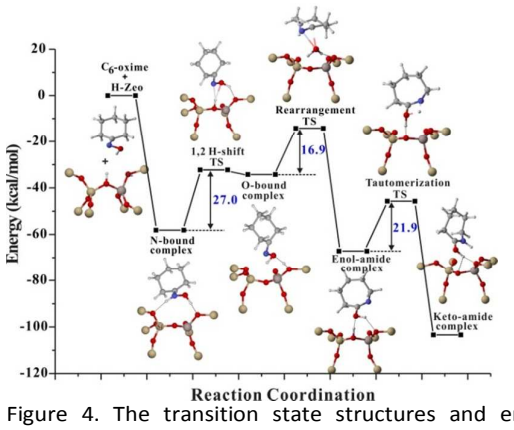

Figure 4. The transition state structures and energy profiles for the cyclohexanone oxime Beckmann rearrangement over the confined pores inside Al-ZSM-5 zeolite.

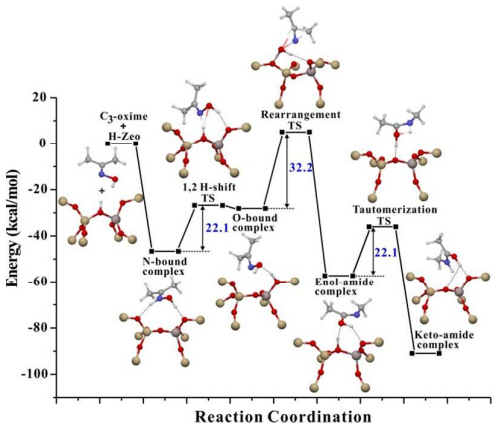

Figure 5. The transition state structures and energy profiles for the acetoxime Beckmann rearrangement over the confined pores inside Al-ZSM-5 zeolite.

determination step in the weak and mediate strong acid strength range (273 <DPE< 319 kcal/mol) , while the 1,2-H shift step becomes the rate-determination step in the strong acid strength range (DPE < 273 kcal/mol). Therefore, a solid acid with strong acidity (DPE is ca. 273 kcal/mol), is the most efficient catalysts for the BR reaction of acetoxime. These calculated results are in well consistent with the experimental results of BR reactions over amorphous metal oxides or mesoporous zeolites in which the pore confinement effect is not so pronounced and the acid strength play a key role in determining the BR reactivity. However, for microporous zeolites, their unique pore structure at subnano-scale (i.e., 0.55 nm for ZSM-5 zeolite) usually provides an effectively confined environment to stabilize reaction intermediates and transition states, which will eventually determine the catalytic performance. Therefore, it is highly desirable to investigate the BR reaction inside the confined pores of zeolites.

Theoretical investigations of the effect of zeolite confinement effect on the catalytic performance of Beckmann rearrangement

Figure 4 shows the energy profile of the cyclohexanone oxime BR reaction over the Al-ZSM-5 zeolite represented by a 72T cluster model containing the intersection of 10-membered ring straight and zigzag pore channels (the optimized TS structures are shown in Figure S8). It can be seen from Figure 4 that the activation barriers are 27.0, 16.9 and 21.9 kcal/mol for the 1, 2-H shift, rearrangement and tautomerization steps respectively on the 72T model. For comparison, the corresponding values are 15.5, 35.8, and 24.3 kcal/mol respectively on the 8T model with a r(Si-H)=1.47 Å. It is noteworthy that the 8T model with has a similar acid strength to the 72T model (their DPE are 309.6 and 309.4 kcal/mol, respectively). Obviously, the activation barrier of rate-determination step significantly decreases from 35.8 kcal/mol (corresponding to the rearrangement step on the isolated acid site of 8T model) to 27.0 kcal/mol (the 1, 2-H shift step on the confined acid site of 72T model). This demonstrates that the confinement effect of ZSM-5 zeolite can considerably reduce the activation barrier and eventually enhance the BR catalytic reactivity of cyclohexanone oxime, which is in good agreement with previous[45] and our experimental observation that ZSM-5 zeolites show much more excellent catalytic performance than MCM-41 zeolites with similar heteroatom substitution. Furthermore, the BR reaction of cyclohexanone oxime on the weaker acidic B-ZSM-5 has been theoretically investigated as well. The activation barriers are 23.4, 20.6 and 22.3 kcal/mol for the 1, 2-H shift, rearrangement and tautomerization steps respectively. Apparently, the relatively lower barrier (23.4 kca/mol) of rate-determination step of B-ZSM-5 compared with that of Al-ZSM-5 (27.0 kca/mol) is indicative of its relatively better catalytic performance, which is in good agreement with our catalytic experiments (Figure 1).

Similarly, the BR reaction of small acetoxime in the confined pores of ZSM-5 zeolites was also investigated. As shown in Figure 5, the

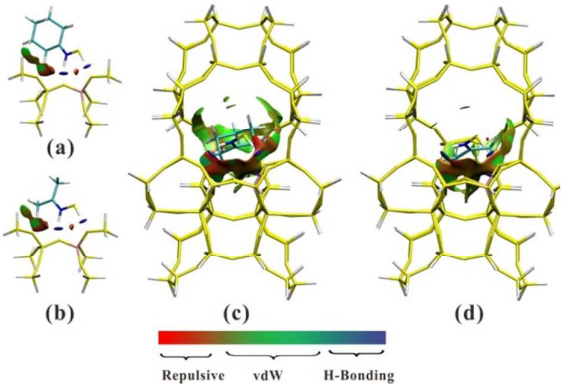

Figure 6. Isosurface plots of reduced density gradient (s=0.500 au) for cyclohexanone oxime (a and c) and acetoxime (b and d) confined in 8T model and ZSM-5 zeolite. The isosurfaces of reduced density gradient were colored according to the values of the quantity sign(λ_2)ρ, and the RGB scale was indicated.

activation barriers are 22.1 (1, 2-H shift), 32.2 (rearrangement step) and 22.1 kcal/mol (tautomerization step) for the BR reaction of acetoxime on the 72T cluster model. For comparison, the corresponding activation barrier of B-ZSM-5 are 19.8, 40.0 and 26.7 kcal/mol respectively. The increased activation barrier (by 7.8 kcal/mol) of rate-determination step confirm that for small acetoxime, weak acidic B-ZSM-5 disfavors but strong acidic Al-ZSM-5 favors the BR reactivity, which is in consistent with our catalytic experiments (Figure 1b). It is interesting to note that the pore structure of ZSM-5 zeolite exhibits different confinement effects on the oximes with different sizes. The estimated dimensions of cyclohexanone and acetoximes are 5.8 × 4.1 $Å^2$ and 4.7 × 2.8 $Å^2$ respectively. Since the dimensional size of the former is comparable to the pore size of ZSM-5 (5.3 × 5.6 $Å^2$), the perfect-fit pore structure of ZSM-5 might provide a strong confinement effect on stabilization of intermdediates or TS species involved in the reaction ofcyclohexanone oxime. It's well known that the visualization of isosurfaces of reduced density gradient in real space is an effective tool to characterize noncovalent interactions between adsorbate and zeolite framework[46]. Figure 6 displays the isosurface of two oximes adsorbed on both isolated 8T and 72T cluster models. On the isolated 8T cluster model, the isosurfaces of two oximes are similar and exclusively located at the local active sites (Figures 6a and 6b). On the 72T cluster model, the larger interaction regions of two oximes confined in H-ZSM-5 zeolite (Figures 6c and 6d) have evidenced the confinement effect from the zeolite framework. Compared to small acetoxime (Figure 6d), the isosurface of cyclohexanone oxime (Figure 6c) displays a much larger green region, being indicative of a stronger van der Waals (vdW) interaction between protonated cyclohexanone oxime and zeolite framework. This results in an improvement of the reactant stability of 1,2-H shift step, which in return leads to a remarkable increase (ca. 11.5 kcal/mol) of the activation energy and makes this step becoming the rate-determination step over the 72T cluster model. However, for the smaller acetoxime, the pore size of ZSM-5 zeolite is too large to provide efficient vdW stabilization (see Fig. 6d) in the zeolite pore structure. As a result, its reaction energy profile is similar to that on the isolated 8T cluster model, in which the rearrangement step is the rate-determination step.

Compared to ZSM-5 zeolite having a channel diameter of ca. 0.55 nm, the relatively large pore size (2.6 nm) of mesoporous MCM-41 could not provide an effective confinement effect on both acetoxime and cyclohexanone oxime, and thus the same trend that the BR reactivity increases with the increase of acid strength of mesoporous zeolites was observed in the catalytic test. This behavior is similar to the BR reactivity versus acid strength on the isolated acid sites as shown in Figure 3. Thus, besides the acid strength, the matching between oxime reactant and zeolite pore plays a crucial role in determining the catalytic reactivity. If the oxime reactant is well-confined inside the pores of zeolites, weaker acid is more favorable to the BR reaction. On the contrary, if the confinement effect is not so pronounced, stronger acid is more favorable to the BR reaction regardless of microporous/mesoporous zeolites or amorphous metal oxide catalysts, which is similar to the case of homogeneous catalysis.

Conclusions

In combination with catalytic experiments and theoretical calculations, the dependence of BR reaction activity on solid acid catalysts properties (e.g., acidic strength and pore structure) has been revealed. It is demonstrated that the different dependence of BR reactivity of different oxime on the acid strength over microporous/mesoporous zeolites is originated from the pore confinement effect. The confinement effect imposed by the microporous zeolite framework has more significant influence on the rate-determination step of BR reaction when the oxime reactant is well-confined inside the microporous voids, which in return controls the catalytic performance.

Acknowledgements

We are grateful for the financial support of the National Natural Science Foundation of China (No. 21173255, 21210005 21173255 and 21403290) and Natural Science Foundation of Hubei Province of China (2014CFA043).

Notes and references

1 K. J. E., R. S., *Handbook of Industrial Chemical, 8th edn., van Nostrand, New York* **1983**, 402.
2 C. Ngamcharussrivichai, P. Wu, T. Tatsumi, *Appl. Catal. A: Gen.* **2005**, *288*, 158-168.
3 L. X. Dai, R. Hayasaka, Y. Iwaki, K. A. Koyano, T. Tatsumi, *Chem. Commun.* **1996**, 1071-1072.
4 M. Anilkumar, W. F. Hoelderich, *Catal. Today* **2012**, *198*, 289-299.
5 M. Anilkumar, W. F. Hoelderich, *Appl. Catal. B: Environ.* **2015**, *165*, 87-93.
6 C. Tagusagawa, A. Takagaki, K. Takanabe, K. Ebitani, S. Hayashi, K. Domen, *J. Catal.* **2010**, *270*, 206-212.
7 Z. Wang, J. Yu, R. Xu, *Chem. Soc. Rev.* **2012**, *41*, 1729-1741.
8 A. Corma, *Chem. Rev.* **1997**, *97*, 2373-2419.
9 A. Corma, A. Martinez, *Adv. Mater.* **1995**, *7*, 137-144.
10 S. Schallmoser, T. Ikuno, M. F. Wagenhofer, R. Kolvenbach, G. L. Haller, M. Sanchez-Sanchez, J. A. Lercher, *J. Catal.* **2014**, *316*, 93-102.
11 F. N. Naraschewski, A. Jentys, J. A. Lercher, *Top. Catal.* **2011**, *54*, 639-649.
12 C. C. Pavel, R. Palkovits, F. Schüth, W. Schmidt, *J. Catal.* **2008**, *254*, 84-90.
13 B. M. Reddy, G. K. Reddy, K. N. Rao, L. Katta, *J. Mol. Catal. A: Chem.* **2009**, *306*, 62-68.
14 J. Sirijaraensre, T. N. Truong, J. Limtrakul, *J. Phys. Chem. B* **2005**, *109*, 12099-12106.
15 H. Kath, R. Gläser, J. Weitkamp, *Chem. Eng. Technol.* **2001**, *24*, 150-153.
16 D. Mao, G. Lu, Q. Chen, *React. Kinet. Catal. Lett.* **2002**, *75*, 75-80.
17 B. Wang, Y. Gu, C. Luo, T. Yang, L. Yang, J. Suo, *Tetrahedron Lett.* **2004**, *45*, 3369-3372.

18 X. Wang, C. C. Chen, S. Y. Chen, Y. Mou, S. Cheng, *Appl. Catal. A: Gen.* **2005**, *281*, 47-54.

19 E. Cano-Serrano, J. M. Campos-Martin, J. L. G. Fierro, *Chem. Commun.* **2003**, 246-247.

20 G. A. Fois, G. Ricchiardi, S. Bordiga, C. Busco, L. Dalloro, G. Spanò, A. Zecchina, in *Stud. Surf. Sci. Catal.* **2001**, *135*, 149.

21 V. R. R. Marthala, Y. Jiang, J. Huang, W. Wang, R. Gläser, M. Hunger, *J. Am. Chem. Soc.* **2006**, *128*, 14812-14813.

22 E. Gianotti, M. Manzoli, M. E. Potter, V. N. Shetti, D. Sun, J. Paterson, T. M. Mezza, A. Levy, R. Raja, *Chem. Sci.* **2014**, *5*, 1810-1819.

23 C. Ngamcharussrivichai, P. Wu, T. Tatsumi, *J. Catal.* **2005**, *235*, 139-149.

24 B. Thomas, S. Sugunan, *Microporous Mesoporous Mater.* **2006**, *96*, 55-64.

25 S. Li, A. Zheng, Y. Su, H. Zhang, L. Chen, J. Yang, C. Ye, F. Deng, *J. Am. Chem. Soc.* **2007**, *129*, 11161-11171.

26 A. Zheng, H. Zhang, L. Chen, Y. Yue, C. Ye, F. Deng, *J. Phys. Chem. B* **2007**, *111*, 3085-3089.

27 G. J. Kramer, R. A. Vansanten, C. A. Emeis, A. K. Nowak, *Nature* **1993**, *363*, 529-531.

28 X. Zheng, P. Blowers, *J. Mol. Catal. A: Chem.* **2005**, *229*, 77-85.

29 H. Van Koningsveld, H. Van Bekkum, J. C. Jansen, *Acta Crystallogr. B* **1987**, *43*, 127-132.

30 B. Han, Y. Chu, A. Zheng, F. Deng, *Acta Phys. Chim. Sin.* **2012** *28*, 315.

31 M. J. Frisch, G. W. Trucks, H. B. Schlegel, G. E. Scuseria, M. A. Robb, J. R. Cheeseman, G. Scalmani, V. Barone, B. Mennucci, G. A. Petersson, H. Nakatsuji, M. Caricato, X. Li, H. P. Hratchian, A. F. Izmaylov, J. Bloino, G. Zheng, J. L. Sonnenberg, M. Hada, M. Ehara, K. Toyota, R. Fukuda, J. Hasegawa, M. Ishida, T. Nakajima, Y. Honda, O. Kitao, H. Naka, T. Vreven, J. A. Montgomery, J. E. Peralta, F. Ogliaro, M. Bearpark, J. J. Heyd, E. Brothers, K. N. Kudin, V. N. Staroverov, R. Kobayashi, J. Normand, K. Raghavachari, A. Rendell, J. C. Burant, S. S. Iyengar, J. Tomasi, M. Cossi, N. Rega, J. M. Millam, M. Klene, J. E. Knox, J. B. Cross, V. Bakken, C. Adamo, J. Jaramillo, R. Gomperts, R. E. Stratmann, O. Yazyev, A. J. Austin, R. Cammi, C. Pomelli, J. W. Ochterski, R. L. Martin, K. Morokuma, V. G. Zakrzewski, G. A. Voth, P. Salvador, J. J. Dannenberg, S. Dapprich, A. D. Daniels, O. Farkas, J. B. Foresman, J. V. Ortiz, J. Cioslowski, G. D. J. Fox, W. Inc., *Gaussian 09, Revision B.01* **2010**.

32 E. R. Johnson, S. Keinan, P. Mori-Sánchez, J. Contreras-García, A. J. Cohen, W. Yang, *J. Am. Chem. Soc.* **2010**, *132*, 6498-6506.

33 T. Lu, F. Chen, *J. Comput. Chem.* **2012**, *33*, 580-592.

34 Q. Luo, F. Deng, Z. Yuan, J. Yang, M. Zhang, Y. Yue, C. Ye, *J. Phys. Chem. B* **2003**, *107*, 2435-2442.

35 V. Sundaramurthy, I. Eswaramoorthi, N. Lingappan, *Can. J. Chem.* **2004**, *82*, 631-640.

36 V. Van Speybroeck, J. Van der Mynsbrugge, M. Vandichel, K. Hemelsoet, D. Lesthaeghe, A. Ghysels, G. B. Marin, M. Waroquier, *J. Am. Chem. Soc.* **2010**, *133*, 888-899.

37 G. Yang, B. Schäffner, M. Blug, E. J. M. Hensen, E. A. Pidko, *ChemCatChem* **2014**, *6*, 800-807.

38 N. Hansen, R. Krishna, J. M. van Baten, A. T. Bell, F. J. Keil, *J. Phys. Chem. C* **2009**, *113*, 235-246.

39 C. Tuma, T. Kerber, J. Sauer, *Angew. Chem. Int. Ed.* **2010**, *49*, 4678-4680.

40 C. S. Yang, J. M. Mora-Fonz, C. R. A. Catlow, *J. Phys. Chem. C* **2013**, *117*, 24796-24803.

41 A. B. Fernández, M. Boronat, T. Blasco, A. Corma, *Angew. Chem. Int. Ed.* **2005**, *44*, 2370-2373.

42 G. Yang, E. A. Pidko, E. J. M. Hensen, *Chemsuschem* **2013**, *6*, 1688-1696.

43 M. T. Nguyen, G. Raspoet, L. G. Vanquickenborne, *J. Chem. Soc., Perkin Trans. 2* **1995**, 1791-1795.

44 J. Macht, M. J. Janik, M. Neurock, E. Iglesia, *Angew. Chem. Int. Ed.* **2007**, *46*, 7864-7868.

45 A. B. Fernández, I. Lezcano-Gonzalez, M. Boronat, T. Blasco, A. Corma, *J. Catal.* **2007**, *249*, 116-119.

46 C. Wang, Y. Chu, A. Zheng, J. Xu, Q. Wang, P. Gao, G. Qi, Y. Gong, F. Deng, *Chem. A Eur. J.* **2014**, *20*, 12432-12443.

Table of Contents (TOC)

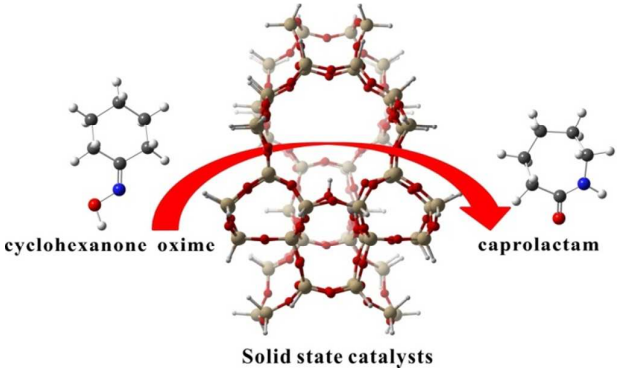

The effects of Brønsted acid strength and pore confinement on the Beckmann rearrangement reaction over solid acid catalysts have been explored.